Progress In Electromagnetics Research, PIER 85, 425–438, 2008

ANALYSIS OF MULTILAYERED CYLINDRICAL STRUCTURES USING A FULL WAVE METHOD

N. Ammar and T. Aguili

Laboratory of System Communications in Engineering School of Tunis (ENIT)
Bélévédère, BP 37, Tunis 1002, Tunisia

H. Baudrand

Electronics Laboratory LEN7
ENSEEIHT
2 rue Camichel, Toulouse 31071, France

Abstract—In this paper, Wave Concept Iterative Procedure (WCIP) is used to investigate scattering by multilayered cylindrical structures in free space and to calculate the diffracted far field by adopting a cylindrical coordinate formulation. The WCIP principle consists of alternating waves between the modal and space domains. Its iterative resolution process is always convergent in lossless media case. The proposed technique used for determining the electric far field diffracted by a multilayered cylindrical structure is validated and confronted to literature results.

1. INTRODUCTION

The electromagnetic analysis of cylindrically layered media is important as it is widely used in many engineering applications. An understanding of the scattering by multilayered structures is imperative in order to take account of its interference and coupling effect with other components. Several studies have been performed for the analysis of electromagnetic and optical scattering of layered cylinders composed of isotropic and anisotropic materials and also arrays of such structures in various configurations. Among those techniques are the integral equation formulation, partial differential equation formulation, and hybrid techniques [1–7].

In this paper, we employ the fullwave [8–10] iterative process theory for the computation of the diffracted far field for multilayered circular cylindrical objects. The WCIP principle consists of expressing the boundary and closing conditions in terms of incident and scattered waves related by a bounded diffraction operator. The WCIP avoids the undesired phenomenon of unbounded operators; relations between currents and fields, obtained using unbounded impedance operators, are transposed to relations between waves, supplied by bounded scattering operators [11]. The modulus of the modal coefficients of the scattering operators is less than unity, which is not the case for the modal coefficients of the impedance operators. The method's convergence is therefore always guaranteed [12]. The power of the WCIP was first verified in the analysis of planar circuits by Akatimagool et al. [13] and Wane et al. [14]. The extension of the procedure to scattering by small cylinders can be seen in [15–17]. The results obtained from using the WCIP on planar circuits have been validated by comparison to measurements and the use of other simulations methods [13, 14]. We will now attempt to extend the use of WCIP to cylindrical systems.

This paper is organized as follows: Section 2 provides a theoretical formulation of the WCIP approach and outlines how the cylindrical formulation of the integral equations solves successfully the scattering multilayered cylindrical structure. In Section 3, the validation of the proposed approach is performed by comparing its results with those in technical literature. Finally, the conclusive remarks are presented in Section 4.

2. THEORETICAL FORMULATION

Figure 1 shows an infinitely long conducting or dielectric circular cylinder of radius 'R_1' with its axis coincident with the z axis. There are several coaxial cylindrical media layers with radii 'R_2', 'R_3', ..., R_p. The structure is placed in free space (ε_0, μ_0) and the time dependence is assumed as e^{-jwt}. A TE (with $E_z = 0$) or TM (with $H_z = 0$) polarized plane wave is normally incident on the multilayered cylindrical structure.

2.1. WCIP Theory

The formulation of the iterative method has been described in [11–18]. It is based on the wave concept, which is introduced by writing the tangential (in each interface Ω_j) electric and magnetic fields, in terms of outgoing ($\vec{A}_i^j$) and incoming ($\vec{B}_i^j$) waves (Fig. 1). It leads to the

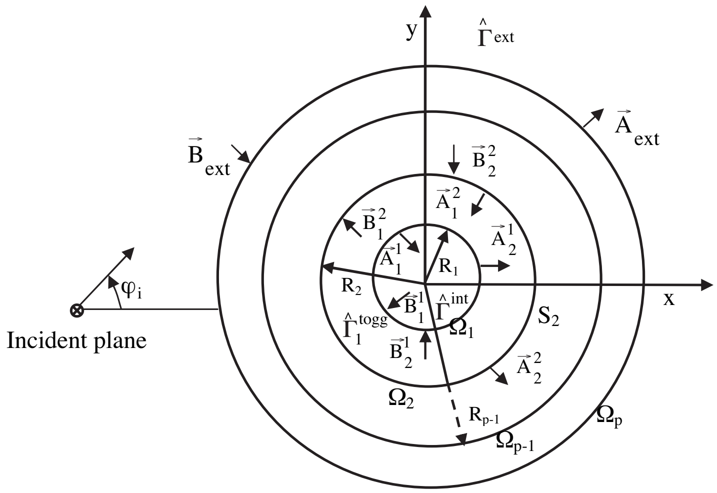

Figure 1. Multilayered cylindrical structure and definition of the waves.

following set of equations:

$$\begin{cases} \vec{A}_i^j = \dfrac{1}{2\sqrt{Z_{0i}^j}}\left(\vec{E}_i^j + Z_{0.i}^j \vec{H}_i^j \wedge \vec{n}_j\right) \\ \vec{B}_i^j = \dfrac{1}{2\sqrt{Z_{0i}^j}}\left(\vec{E}_i^j - Z_{0.i}^j \vec{H}_i^j \wedge \vec{n}_j\right) \end{cases} \tag{1}$$

with

the subscript i refer to media 1 and 2 divided by the interface Ω_j.

z_{0i}^j: the intrinsic impedance of medium i for each interface j.

j: order of interface.

$\vec{n}_j$: a unit vector normal to interface Ω_j.

For reason of clarity, the surface current density is introduced:

$$\vec{J}_i^j = \vec{H}_T \wedge \vec{n}_j \tag{2}$$

By the same way, the transverse electromagnetic fields on each of the two sides of the interface Ω_j can be deduced from the waves by:

$$\begin{cases} \vec{E}_i^j = \sqrt{Z_{0.i}^j}\left(\vec{A}_i^j + \vec{B}_i^j\right) \\ \vec{J}_i^j = \dfrac{1}{\sqrt{Z_{0.i}^j}}\left(\vec{A}_i^j - \vec{B}_i^j\right) \end{cases} \tag{3}$$

Each homogenous layer of order j, in Fig. 1, $(1 < j < P)$, between interface j and $j+1$ is characterized by the toggling operator $\Gamma_{\text{togg}}^{(j,j+1)}$ [19] relating the incoming and outgoing waves following:

$$\begin{bmatrix} B_2^j \\ B_1^{j+1} \end{bmatrix} = \Gamma_{\text{togg}}^{(j,j+1)} \begin{bmatrix} A_2^j \\ A_1^{j+1} \end{bmatrix} \tag{4}$$

For the operators $\hat{\Gamma}^{\text{ext}}$ and $\hat{\Gamma}^{\text{int}}$, respectively, associated to the exterior and interior layers, Equation (4) is rewritten as:

$$\begin{cases} \vec{B}_1^1 = \hat{\Gamma}^{\text{int}} \vec{A}_1^1 \\ \vec{B}_2^P = \hat{\Gamma}^{\text{ext}} \vec{A}_2^P \end{cases} \tag{5}$$

with

$\hat{\Gamma}_{\text{ext}}$: External diffraction operator modeling the wave behaviour in the outer region of the cylinder for radius R_p [15, 16, 19].

$\hat{\Gamma}_{\text{int}}$: Internal diffraction operator modeling the wave behaviour in the interior region of the cylinder for radius R_1 [15, 16, 19].

The concept of toggling operator permits us to investigate the modeling of wave penetration into multilayered cylindrical media by generating a network representation of the wave formalism. This can be performed by defining a toggling operator for every two neighboring media besides the internal and external operators corresponding respectively to the inner and outer region of the global multilayered structure.

More generally, in the spectral domain, the incoming and the outgoing waves are linked in each other by the following relation:

$$\vec{B} = \hat{\Gamma} \vec{A} \tag{6}$$

For the multilayered structure in Fig. 1, the condensed Equation (6) is developed as fellow:

$$\begin{vmatrix} B_2^1 \\ B_1^1 \\ B_1^2 \\ \vdots \\ \vdots \\ B_2^{j-1} \\ B_1^j \\ \vdots \\ \\ B_P^2 \end{vmatrix} = \begin{vmatrix} \hat{\Gamma}_{\text{int}} & & & & & \\ & \left[\Gamma_{\text{togg}}^{(1,2)}\right] & & & & \\ & & \ddots & & & \\ & & & \left[\Gamma_{\text{togg}}^{(j-1,j)}\right] & & \\ & & & & \ddots & \\ & & & & & \Gamma_{\text{ext}} \end{vmatrix} \begin{vmatrix} A_2^1 \\ A_1^1 \\ A_1^2 \\ \vdots \\ \vdots \\ A_2^{j-1} \\ A_1^j \\ \vdots \\ \\ A_P^2 \end{vmatrix} \tag{7}$$

In the spectral domain, the modal expansion of the reflection operator following the Dirac notation is given by:

$$\hat{\Gamma}_{\sigma}^{\alpha} = \sum_{n} \left| f_{n,R_1}(\varphi, z) \right\rangle \Gamma_{\sigma \cdot n}^{\alpha} \left\langle f_{n,R_2}\left(\varphi', z'\right) \right| \tag{8}$$

where:

(φ, z) the observation point.

(φ', z') the excitation point.

$\Gamma_{\sigma \cdot n}^{\alpha}$ is the modal coefficient of the diffraction operator.

The subscript σ designate: togg, ext or int and the subscript α refer to the TM or TE polarizations.

R_1 and R_2 are respectively cylindrical radius where are defined the outgoing and the incoming waves $\vec{A}$ and $\vec{B}$.

$f_{n,R_k} = \frac{1}{\sqrt{2\pi R_k}} e^{jn\varphi}$: The common modal basis function for both TE and TM modes describing a cylinder of radius R_k.

On the other hand, the space scattering operator is deduced from the continuity of fields and the boundary conditions on each sub domain of Ω_j. At the discontinuity interface Ω_j, enforcing the continuity conditions of the electromagnetic fields ($E_{t1} = E_{t2}$ and $J_1 + J_2 = 0$ on the dielectric domain and $E_{t1} = E_{t2} = 0$ on the metallic domain) and taking into account the definition of the waves in (1), the outgoing and the incoming waves are linked in the spatial domain by the following relation:

$$\begin{bmatrix} \vec{A}_2^j \\ \vec{A}_1^j \end{bmatrix} = \hat{S}^j \cdot \begin{bmatrix} \vec{B}_2^j \\ \vec{B}_1^j \end{bmatrix} \tag{9}$$

with

$$\hat{S}^j = \begin{bmatrix} -\dfrac{\eta_j^2 - 1}{\eta_j^2 + 1} H_D^j - H_M^j & \dfrac{2\eta_j^2}{\eta_j^2 + 1} H_D^j \\ \dfrac{2\eta_j^2}{\eta_j^2 + 1} H_D^j & \dfrac{\eta_j^2 - 1}{\eta_j^2 + 1} H_D^j - H_M^j \end{bmatrix} \tag{10}$$

where

$H_M^j = 1$ on the metal of interface j and 0 elsewhere.

$H_D^j = 1$ on the dielectric of interface j and 0 elsewhere.

$$\eta_j = \sqrt{\frac{z_{0.1}^j}{z_{0.2}^j}} \tag{11}$$

One takes account of different interfaces (j) of the structure in Fig. 1, the boundary conditions is expressed as fellows:

$$\begin{vmatrix} A_1^1 \\ A_2^1 \\ A_1^2 \\ A_2^2 \\ \vdots \\ A_1^k \\ A_2^k \\ \vdots \\ A_1^p \\ A_2^p \end{vmatrix} = \begin{vmatrix} \left[\hat{S}^1\right] & & & & & \\ & \left[\hat{S}^2\right] & & & & \\ & & \ddots & & & \\ & & & \left[\hat{S}^k\right] & & \\ & & & & \ddots & \\ & & & & & \left[\hat{S}^p\right] \end{vmatrix} \begin{vmatrix} B_1^1 \\ B_2^1 \\ B_1^2 \\ B_2^2 \\ \vdots \\ B_1^k \\ B_2^k \\ \vdots \\ B_1^p \\ B_2^p \end{vmatrix} \tag{12}$$

Equation (12) as rewritten in condensed form as fellow:

$$\vec{A} = \hat{S}\vec{B} \tag{13}$$

2.2. Iterative Process

Collecting the waves from (6) and (13), results in a set of coupled equations summarizing the continuity conditions in the spatial domain and integral relations in the spectral domain. In presence of the plane wave excitation, the iterative scheme is initialized by the excitations waves corresponding to the incident tangential electromagnetic fields.

At iteration k, the iterative solution is governed by the following equation system:

$$\begin{cases} \vec{A}^{(k)} = \hat{S}\vec{B}^{(k-1)} + \delta_p^j f\left(\vec{A}_0, \vec{B}_0\right) \\ \vec{B}^{(k)} = \hat{\Gamma}\vec{A}^{(k)} \end{cases} \tag{14}$$

where δ_p^j is the kronecker delta,

$$f\left(\vec{A}_0, \vec{B}_0\right) = \begin{bmatrix} -\dfrac{\eta_j^2 - 1}{\eta_j^2 + 1} \cdot \vec{B}_0 H_D^j - \vec{B}_0 H_M^j - \vec{A}_0 \\ \dfrac{2\eta_j^2}{\eta_j^2 + 1} \cdot \vec{B}_0 H_D^j \end{bmatrix} \tag{15}$$

$\vec{A}_0$ and $\vec{B}_0$ are the excitation incident and scattered waves, related to the incident electric field $\vec{E}^{\text{inc}}$ and $\vec{J}^{\text{inc}}$ current density by using the relation (1).

The toggling between the spectral and the spatial domains is ensured by the fast Fourier transform and this inverse.

The iterative process (14) is stopped when both the norms $\left\|\Delta\vec{A}_k\right\|$ and $\left\|\Delta\vec{B}_k\right\|$ tend to zero. In the convergence of the iterative process, the current density and the tangential electric field can be computed in each interface j.

2.3. Diffracted Far Field

The WCIP solution of the far-field scattered is carried out in two steps:

-Step 1: Computation of the electromagnetic near field's on the exterior interface of the structure (courant density and the tangential electric field).

-Step2: When the convergence of current density or electric fields at the exterior interface is attained, the outgoing exterior waves $\vec{A}_{\text{ext}}$ are transformed at the far zone in order to calculate the tangential diffracted far field on a fictitious cylinder with electrically large radius ($\rho \gg \lambda$) (Fig. 2).

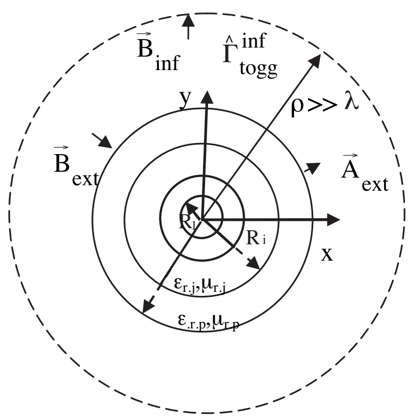

Figure 2. Schema of diffracted far field.

It is worth noting that this transformation is ensured by using the asymptotic development of the expressions of the toggling operator $\hat{\Gamma}_{\text{togg}}$. We denoted by $\hat{\Gamma}^{\text{inf}}_{\text{togg}}$ this asymptotic value.

2.4. WCIP Method Versus the Method of Moments (MOM)

A numerical evaluation of the WCIP CPU run time is presented to show the efficiency of the method when handling largely metalled structures.

Let N be the number of pixels and n_it the number of iterations, the total number of operations $N_{\text{op-WCIP}}$ for a simulation is given by $N_{\text{op-WCIP}} = n\_\text{it} * 4N(1 + 3\ln N)$.

n_it, on the order of 50, to reach the convergence of the WCIP iterative process for 2D structure.

Since $4N$ operations are needed in the spatial domain because of the two components at each pixel and $12N\log_e N$ operations are performed in the fast Fourier transform and their inverse (FFT and FFT^{-1}) at each iteration.

P is the number of pixels used to describe the interface.

In the method of moments (MOM), the number of operations $N_{\text{op-MOM}}$ can be calculated using [18]:

$$N_{\text{op-MOM}} = \frac{P^3}{3} \tag{16}$$

To do comparison between the MOM method and the WCIP method in terms of running time, P is also taken as the number of pixels used to define the metallic domain of each interface j. Thus P can be related to N by:

$$N = KP \tag{17}$$

with k being the ratio between the metallic part of the interface j and all the interface.

In Fig. 2, the number of multiplications for a different numbers of iteration is compared, in the case of a single interface, to the evolution of $N_{\text{op-MOM}}$ against m.

One can conclude that for a large metalized structure (requiring a significant number of metal cells) $k < 10$, the $N_{\text{op-WCIP}}$ is far less than the $N_{\text{op-MOM}}$. Therefore, in this case, the WCIP algorithm is obviously superior to the MoM implementation in terms of execution time.

3. NUMERICAL RESULTS

In this section, some numerical examples are presented to demonstrate the applicability of the WCIP for analyzing largescale electromagnetic scattering of multilayered cylindrical structures.

The first example, we consider a dielectric cylinder with permittivity relative ε_{r1} is covered of a dielectric coating of permittivity relative ε_{r2}; the configuration is illustrated in Fig. 4.

The geometrical parameters are: $R_2 = 2.5\lambda$; $R_1 = 2\lambda$. The dielectric permittivity are: $\varepsilon_{r1} = 9$; $\varepsilon_{r2} = 4$; $\varepsilon_{r3} = 1$. The studied

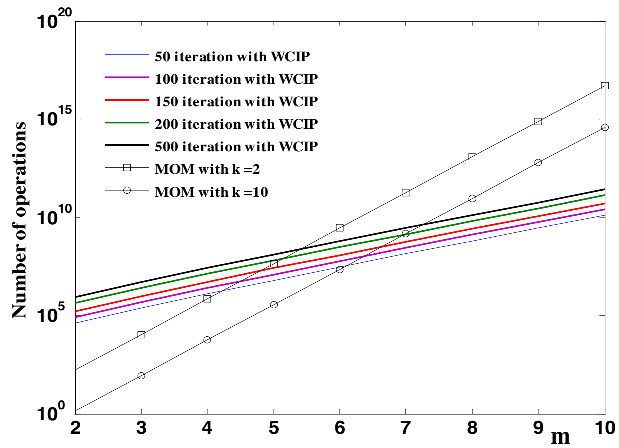

Figure 3. Computational cost.

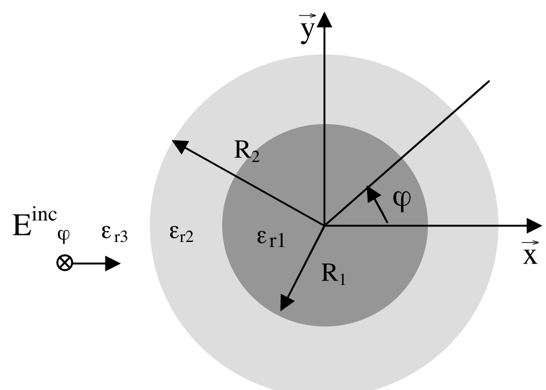

Figure 4. Circular dielectric coated cylinder.

structure excited by a TE plane wave under normal incidence. We simulate this structure with 2^7 resolution.

At the convergence of the exterior near electric field (Fig. 5), when the iterative process is achieved after 25 iterations, the induced current on the external cylinder (at $R = R_2$) is shown in Fig. 6. It is clear that the current density distribution is null on the dielectric interface. In fact, the boundary condition of the tangential current on the dielectric region is respected, which proves the consistence of our approach.

The normalised scattering far field (to the incident field), calculated using the above WCIP formulation, is diagrammed in Fig. 7.

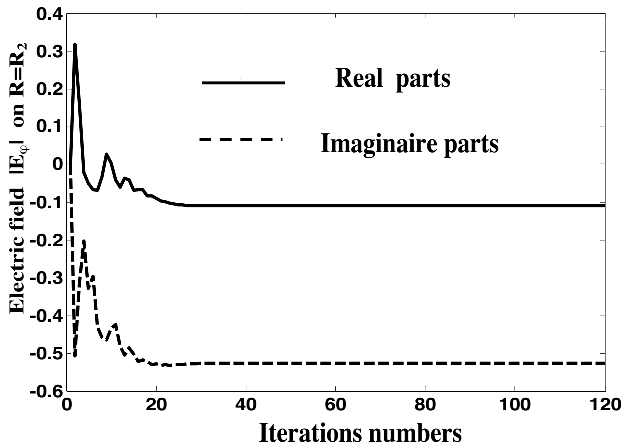

Figure 5. Convergence of the iterative process.

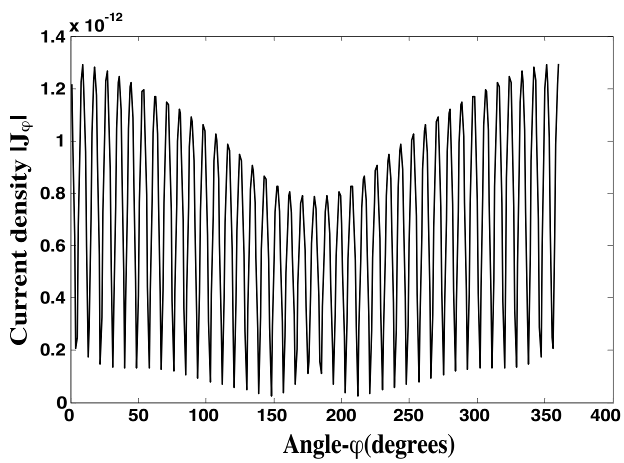

Figure 6. Current density at $\rho = R_2$.

The results obtained using WCIP is compared to the one calculated by the integral equation in [20]. It can be seen that the agreement between the two results is good.

The second example we consider is a single dielectric cylinder with air core. The inner radius of the cylinder is $a = 0.25\lambda$ and the outer radius is $b = 0.3\lambda$, having relative permittivity $\varepsilon_r = 4$, excited by a TM plane wave, with incidence angle $\varphi_i = 0$. The resolution numbers is 2^5.

The radar cross section represents a convenient way to describe

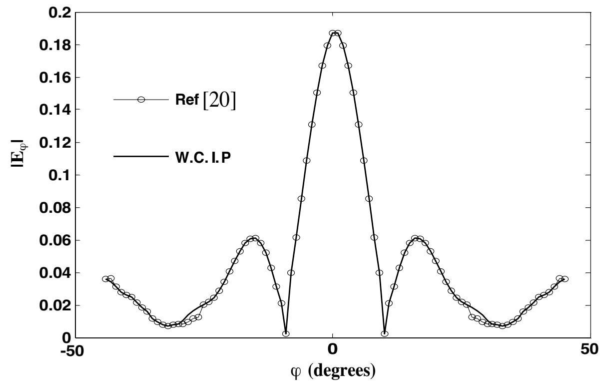

Figure 7. Normalized scattering far field.

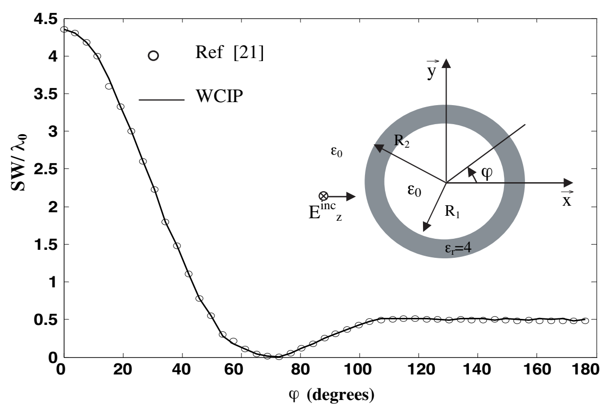

Figure 8. Plots of the normalized SW versus the observation angle for a dielectric cylindrical shell.

the strength of scattered fields observed in the far fields. For 2-D objects like infinite cylinders, the RCS becomes the scattering width (SW) defined by:

$$\mathrm{SW} = \lim_{\rho \to \infty} \left[2\pi\rho \frac{|E^{\mathrm{sc}}|^2}{|E^{\mathrm{inc}}|^2} \right] \tag{18}$$

In Fig. 8, the normalized SW (to the wave length λ_0 of the incident wave) plots versus the observation angle φ are given for a single cylindrical shell. The result generated using the WCIP method is compared to the SW data based on the method of moment solution presented in [21]. It is clear from the figure that the two solutions are in complete agreement.

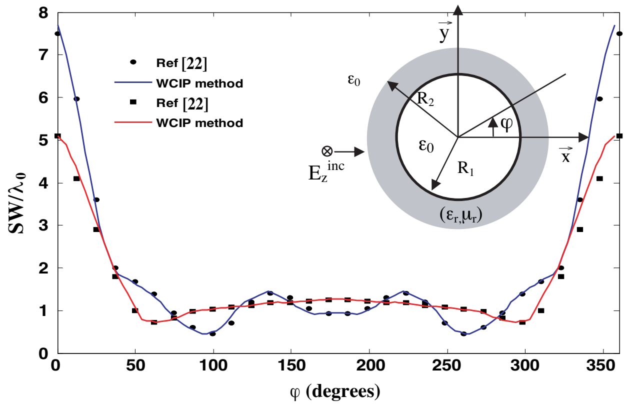

Figure 9. Plots of the normalized SW versus the observation angle of a single conducting cylinder coated with either dielectric or metamaterial.

For the third example, we consider a single coated conducting cylinder, the coating layer was made of a dielectric material having relative permittivity of $\varepsilon_r = 9.8$ and $\mu_r = 1$ or a metamaterial having relative permittivity $\varepsilon_r = -9.8$ and relative permeability $\mu_r = -1$ (Fig. 9).

The metamaterial parameters used in this paper are selectively used to provide confirmation of the validity of the WCIP formulation by comparison of special cases with published results. For comparison, the incident wave frequency is set to 1 GHz, the radius of the conducting cylinder is $R_1 = 0.05\lambda$, the outer radius of the coating cylinder is $R_2 = 0.1\lambda$, and excited by a TMz plane wave with incident angel $\varphi_i = 0$. Fig. 9 represents also the SW normalized to wave length λ_0 of the incident plane wave; the results show a complete agreement with the independently reported results in [22].

4. CONCLUSIONS

In this work, an original integral method based on a transverse wave formulation has been applied successfully to calculate the radar cross section of 2D structure. A cylindrical local basis function is used in the modal expansion of the diffraction operators involved in the resolution of scattering problem by multilayered cylinder. The computation of the scattered far field was performed thanks to an original concept of fictitious cylinder. A good agreement with technical literature was observed which proves the efficiency of the present method.

REFERENCES

1. Zhang, M., T. S. Yeo, L. W. Li, and M. S. Leong, "Electromagnetic scattering by a multilayer gyrotropic bianisotropic circular cylinder," *Progress In Electromagnetics Research*, PIER 40, 91–111, 2002.
2. Kolawole, M. O., "Scattering from dielectric cylinders having radially layered permittivity," *J. Electromagn. Waves Applicat.*, Vol. 6, 235–259, 1992.
3. Vecchia, D., L. Guerriero, I. Bruni, and P. Ferrazzoli, "Hollow cylinder microwave model for STEMS," *J. of Electromagn. Waves and Applicat.*, Vol. 20, No. 3, 301–318, 2006.
4. Valagiannopoulos, C. A., "Arbitrary currents on circular cylinder with inhomogeneous cladding and RCS optimization," *J. of Electromagn. Waves and Applicat.*, Vol. 21, No. 5, 665–680, 2007.
5. Zhong, X.-M., C. Liao, andW. Chen "Image reconstruction of arbitrary cross section conducting cylinder using UWB pulse," *J. of Electromagn. Waves and Appl.*, Vol. 21, No. 1, 25–34, 2007.
6. Abd-El-Raouf, H. E. and R. Mittra, "Scatering analysis of dielectric coated cones," *J. of Electromagn. Waves and Appl.*, Vol. 21, No. 13, 1857–1871, 2007.
7. Yin, W. Y., L. W. Li, and M. S. Leong, "Scattering from multiple bianisotropic cylinders and their modeling of cylindrical objects of arbitrary cross-section," *Progress In Electromagnetics Research*, PIER 27, 159–184, 2000.
8. Oraizi, H. and A. Abdolali, "Ultra wide bande RCS optimization of multilayered cylindrical structures for arbitrarily incident plane wave," *Progress In Electromagnetics Research*, PIER 78, 129–157, 2008.
9. Anastassiu, H. T., "Error estimation of the method of auxiliary sources (MAS) for scattering from an impedance circular cylinder," *Progress In Electromagnetics Research*, PIER 52, 109–128, 2005.
10. Hill, S. C. and J. M. Jarem, "Scattering of multilayer concentric elliptical cylinders excited by single mode source," *Progress In Electromagnetics Research*, PIER 55, 209–226, 2005.
11. Baudrand, H. and D. Bajon, "Equivalent circuit representation for integral formulation of electromagnetic problems," *Int. J. Numer., Model. Electron.*, 23–57, Netw. Devices Fields, January 15, 2002.
12. Baudrand, H. and R. S. N'Gongo, "Application of wave concept iterative procedure," *Recent Research Developments in Microwave Theory and Techniques*, Vol. 1, 187–197, Transworld Research

Network, Kerala, India, 1999.

13. Akatimagool, S., D. Bajon, and H. Baudrand, "Analysis of multilayer integrated inductors with wave concept iterative procedure (WCIP)," *IEEE MTT-S Proc. Int. Microw. Symp. Dig.*, Vol. 3, 1941–1944, May 2001.
14. Wane, S., D. Bajon, and H. Baudrand, "Fullwave analysis of stacked structures including inhomogeneous layers. Hybrid integral-differential approach in terms of waves," *Proc. New Trends and Concepts in Microwave Theory and Techniques Conf.*, 131–166, February 2003.
15. Raveu, N., T. P. Vuong, I. Terrasse, G.-P. Piau, and and H. Baudrand, "Near fields evaluated with the wave concept iterative procedure method for an E-polarisation plane wave scattered by cylindrical strips," *Microwave and Optical Technology Letters*, Vol. 38, No. 05, 403–406, September 2003.
16. Raveu, N., T. P. Vuong, I. Terrasse, G.-P. Piau, G. Fontgalland, and H. Baudrand, "Wave concept iterative procedure applied to cylinders," *IEE Proc. - Microw. Antennas Propag.*, Vol. 151, No. 5, October 2004.
17. Bedira, R., A. Gharsallah, A. Gharbi, and H. Baudrand, "An iterative process based on the concept of waves for electromagnetic scattering problems," *Electromagnetics*, Vol. 22, 129–140, 2002.
18. N'Gongo, R. S. and H. Baudrand, "Application of wave concept iterative procedure in planar circuits," *Recent Res. Devel. Microwave Theory and Technique*, Vol. 1, 187–197, 1999.
19. Ammar, N., T. Bdour, T. Aguili, and H. Baudrand, "Investigation of electromagnetic scattering by arbitrarily shaped structures using the wave concept iterative process," *Journal of Microwaves, Optoelectronics and Electromagnetic Applications*, Vol. 7, No. 1, June 2008.
20. Tsai, C.-C. and S.-T. Wu, "A new single surface integral equation for light scattering by circular dielectric cylinders," *Optics Communications*, Vol. 277, 247–250, 2007.
21. Richmond, J. H., "Scattering by a dielectric cylinder of arbitrary cross-section shape," *IEEE Trans. Antennas Propagat.*, Vol. 13, 334–341, 1965.
22. Li, C. and Z. Shen, "Electromagnetic scattering by a conducting cylinder coated with metamaterials," *Progress In Electromagnetics Research*, PIER 42, 91–105, 2003.